Crystallization of ribozymes and small RNA motifs by a sparse matrix approach

(ribonucleic acids/x-ray crystallography)

Jennifer A. Doudna*†, Cheryl Grosshans‡, Anne Gooding‡, and Craig E. Kundrot*†

*Department of Chemistry and Biochemistry and ‡Howard Hughes Medical Institute, University of Colorado, Boulder, CO 80309-0215

ABSTRACT The three-dimensional structures of RNA enzymes form catalytic centers that include specific substrate binding sites. High-resolution determination of these and other RNA structures is essential for a detailed understanding of the function of RNA in biological systems. The crystal structures of only a few RNA molecules are currently known. These include tRNAs, which were produced *in vivo* and contained modified bases, and short oligonucleotide duplexes lacking tertiary interactions. Here we report that a number of different RNA molecules of 4–50 kDa, all synthesized *in vitro*, have been crystallized. A highly successful method for the growth of RNA crystals based on previously reported conditions for tRNA crystallization is presented. This method is rapid and economical, typically requiring 1.1 mg of RNA to set up an experiment and 2 weeks to complete the observations. Using this technique, we have obtained crystals of 8 of 10 different RNA molecules tested, ranging in size from a dodecamer duplex to a 208-nucleotide catalytic intron. Several of these crystal forms diffract to high resolution; in one case, we have collected a 2.8-Å native data set for a 160-nucleotide domain of the group I self-splicing intron from *Tetrahymena thermophila*. The solution of these RNA structures should reveal aspects of tertiary structure that relate to RNA function and catalytic mechanisms.

The structures of RNA macromolecules are essential to their function in biological systems. Extensive biochemical evidence suggests that RNA enzymes fold to form catalytic centers, which include specific substrate binding sites (1–4). For example, the group I self-splicing introns have defined binding sites for the substrates guanosine and an RNA double helix, and substrate specificity can be altered by making site-directed mutations within the catalytic core of the RNA (5–8). In other cases, RNA structures form specific sites for protein recognition and binding. For example, tRNAs are bound specifically by cognate tRNA synthetases via particular sequence or structural interactions between the RNA and the protein (9, 10). Other well-studied examples include the Tar and Rev-responsive element sites of human immunodeficiency virus type 1 (HIV-1), which form binding sites for key regulatory proteins involved in HIV-1 replication (11–15).

The nature of RNA tertiary structural interactions has been investigated by using genetic and site-directed mutagenesis approaches. In addition, phylogenetic sequence comparison has proved a powerful tool for deduction of likely structural interactions (16, 17). Recently, structural interactions have been identified by *in vitro* selection techniques (18, 19). However, a much more detailed understanding of RNA folding and function will be possible only with the availability of high-resolution crystal structures of these molecules.

The x-ray crystal structures of several tRNA molecules have been determined, and this has yielded extensive information about tertiary contacts in RNA. Triple-base interactions and noncanonical base pairings stabilize the three-dimensional conformation of the molecule and enable it to perform its many functions in the cell (20–23). The cocrystal structure of a tRNA with its cognate tRNA synthetase has revealed protein–RNA contacts that give rise to the specificity of these interactions (10). In addition, two crystal structures of RNA oligonucleotide duplexes have been reported (24, 25).

Despite these advances, however, the study of RNA structure by x-ray crystallography is a relatively new field. Questions remain about the general ability of RNA molecules to be crystallized and the degree of primary and tertiary structural homogeneity required for crystallization. The crystallization of macromolecules is a highly empirical process even for proteins, for which there are now ≈1000 crystal structures known. In the case of RNA macromolecules, additional factors may complicate crystallization, such as the source and purity of material and the inherent instability of RNA. Furthermore, RNA molecules in some cases exist as a set of stable conformers in solution (26–28); conditions that favor the active conformation must be found and applied to the crystallization process.

We have developed a sparse matrix method for the growth of RNA crystals for x-ray diffraction analysis. This approach is based on the earlier incomplete factorial (29) and sparse matrix (30) methods for protein crystallization. Using this technique, we have obtained crystals of 8 of 10 different RNA molecules tested. RNA was produced by both *in vitro* transcription and solid-phase chemical synthesis. These molecules ranged in size from a dodecamer duplex to a 208-nucleotide catalytic intron. After determination of initial crystallization conditions, parameters were optimized to yield crystals appropriate for x-ray diffraction studies.

Perhaps most exciting for the future of RNA structural biology, several of our RNA crystals diffract to high resolution. In particular, we have collected a native data set to 2.8 Å resolution for a 160-nucleotide domain of the group I intron from *Tetrahymena thermophila*.

We believe that our sparse matrix screen will be useful to molecular biologists and crystallographers alike who are seeking to crystallize RNA molecules of interest. The screen is rapid and requires minimal material (1.1 mg). Since it has proven successful for growing crystals of a wide range of RNA molecules in our experience, it is hoped that others may use it to begin work toward high-resolution crystal structures of many more RNAs.

MATERIALS AND METHODS

RNA Preparation and Purification. RNA for crystallization was prepared either by transcription *in vitro* using T7 RNA

Abbreviation: MPD, 2-methyl-2,4-pentanediol.
†To whom reprint requests should be addressed.

Table 1. Crystallization matrix parameters

Precipitant	Mg^{2+}	Polyamine
2-Propanol	MgCl₂	Spermine
PEG 8000	Mg(OAc)₂	Spermidine
(NH₄)₂SO₄	MgSO₄	Other divalent ions
MPD	pH	CaCl₂
Dioxane	5.5	BaCl₂
1,6-Hexanediol	6.0	CoCl₂
Ethanol	6.5	CrCl₂
t-Butyl alcohol	7.0	NiCl₂
Spermine	7.5	CuCl₂
	8.0	SrCl₂

PEG, polyethylene glycol.

polymerase (31) or by solid-phase chemical synthesis (32, 33). Transcription involved an initial set of optimization experiments for each template of interest in order to maximize yield and purity of material. Typical reaction mixtures included 0.5 μM DNA template, 20 mM MgCl₂, 2 mM spermidine, 40 mM Tris·HCl (pH 8.0), 10 mM dithiothreitol (DTT), 0.01% Triton X-100, and 2.5 mM each nucleoside triphosphate. However, in some cases the optimal amounts of various reagents differed from the above values by severalfold. For example, in several cases increased DTT concentrations (up to 40 mM) dramatically improved the yield of full-length RNA in the transcription reaction. Once optimal template, nucleoside triphosphate, DTT, and magnesium concentrations were identified, a large scale transcription reaction mixture of 20–100 ml (total vol) was prepared. The reaction volume was reduced to 2–5 ml in an Amicon stirred ultrafiltration cell or by adding 2 vol of 100% ethanol and precipitating the nucleic acids on dry ice for 60 min (or overnight). RNA was purified from T7 RNA polymerase, abortive transcripts, unincorporated nucleotides, and DNA template by electrophoresis on denaturing polyacrylamide gels, or by size-exclusion chromatography using Sephacryl S-400 (Pharmacia). After purification, RNA was concentrated by dialysis with an Amicon ultrafiltration apparatus and equilibrated into sterile water or buffer by centrifugation using Centricon ultrafiltration centrifuge tubes. Each RNA preparation was checked for purity on ethidium bromide- or silver-stained denaturing polyacrylamide gels. Typically, the RNA contained less than ≈1% contaminating abortive or degradative products. RNA was stored either lyophilized at −20°C or in solution at 4°C. All water and buffers to be used with the RNA were autoclaved and filtered through 0.2-μm filters before use. By following these procedures, hydrolysis of the RNA was not observed, even when stored at 4°C for several months.

RNA Preincubation and Crystallization. RNA for crystallization trials was diluted to 5 mg/ml in 50 mM buffer and 5 mM magnesium chloride (or magnesium sulfate). This solution was then incubated in a heat block at 60°C for 10 min, and the block was turned off, removed from the heating unit, and allowed to cool slowly to room temperature (≈22°C). The solution was spun through a 0.2-μm filter before use in crystallization trials. Before dilution of the preincubated RNA into crystallization drops, the magnesium, polyamine, and other divalent metal ion concentrations were adjusted to those indicated in Table 2. The hanging drop method was used to screen for RNA crystallization using the sparse matrix conditions (34). This method involves suspending 2- to 4-μl droplets over a 1.0-ml reservoir. For convenience, 24-well tissue culture trays were used (Linbro). To maximize search conditions with minimal use of RNA, three droplets were suspended over each reservoir. The drops contained the following amounts of RNA solution and reservoir solution: 2 μl of RNA, 1 μl of reservoir; 2 μl of RNA, 2 μl of reservoir; 1 μl of RNA, 2 μl of reservoir. Identical sets of trays were prepared—one for incubation at 4°C and one for incubation

Table 2. RNA sparse matrix conditions

Condition	Precipitant	$Mg^{2+},$* mM	pH†	Polyamine, mM	Cation (2 mM)
1	15% 2-propanol	20	6.0	Spermine, 0.5	CaCl₂
2	4% PEG 8000	20	6.0	Spermine, 0.5	
3	7% 2-propanol	15	6.5	Spermine, 0.5	BaCl₂
4	3 M AS	20	5.5	Spermine, 0.5	
5	2 M AS	20	7.0	Spermine, 0.5	
6	10% MPD	5	6.5	Spermine, 0.5	
7	2 M AS	10	7.0	Spermine, 0.5	
8	25% MPD	20‡	6.0	Spermine, 0.5	CoCl₂
9	15% dioxane	10	6.5	Spermine, 0.5	
10	25% dioxane	5	7.0	Spermine, 1.0	
11	10% 1,6-hexanediol	20	7.5	Spermine, 1.0	
12	1 M AS	15	7.5	Spermine, 1.0	CoCl₂
13	4% PEG 8000	20	7.5	Spermine, 1.0	
14	2 M AS	20	7.5	Spermine, 1.0	CoCl₂
15	20% ethanol	15	6.5	Spermine, 1.0	
16	7% 2-propanol	5	6.5	Spermine, 1.0	
17	5% dioxane	5	7.5	Spermine, 1.0	
18	8% t-butyl alcohol	15	6.0	Spermine, 1.0	CaCl₂
19	5% dioxane	10	8.0	Spermine, 1.0	
20	15% MPD	20	6.5	Spermine, 1.0	CoCl₂
21	15% 2-propanol	5	6.0	Spermine, 1.0	CaCl₂
22	25% MPD	5	6.5	Spermine, 1.0	CoCl₂
23	5% MPD	10	6.5	Spermine, 1.5	CoCl₂
24	15% MPD	10	7.5	Spermine, 1.5	
25	3 M AS	10§	6.5	Spermine, 1.5	
26	5% MPD	5	7.0	Spermine, 1.5	CrCl₂
27	8% t-butyl alcohol	10	7.5	Spermine, 1.5	NiCl₂
28	25% dioxane	15	7.5	Spermidine, 1.0	
29	5% MPD	20‡	5.5	Spermidine, 1.0	CuCl₂
30	30% dioxane	10	7.0	Spermidine, 1.0	
31	10% t-butyl alcohol	5	7.0	Spermidine, 1.0	
32	2.5 mM spermine	80	7.5	Spermidine, 1.0	
33	15% MPD	10	7.0		CaCl₂
34	3 M AS	10	6.0		
35	25% dioxane	10§	6.5		CaCl₂
36	30% dioxane	10	7.0		BaCl₂
37	7% 2-propanol	5	6.0		
38	15% dioxane	20	6.0		SrCl₂
39	1 M AS	15	7.5		NiCl₂
40	20% ethanol	5	8.0		
41	15% 2-propanol	15	6.0		CuCl₂
42	15% dioxane	5	7.0		
43	20% ethanol	15	6.0		
44	1 M AS	15	7.0		CoCl₂

AS, ammonium sulfate; PEG, polyethylene glycol.
*MgCl₂ unless otherwise indicated.
†Buffered solutions of RNA and reagents at the indicated pH were prepared by using the buffer chemicals listed in Results and Discussion.
‡MgSO₄.
§Mg(OAc)₂.

at 22°C. Results were recorded over the course of several weeks and tabulated according to starting conditions.

RESULTS AND DISCUSSION

Design of Sparse Matrix Conditions. Five parameters were chosen as variables to be explored in our matrix: pH, magnesium ion concentration, polyamines, other divalent metal ions, and precipitating agents (Table 1). Conditions that had been reported for the crystallization of various tRNAs were compiled and analyzed for frequency of use of particular reagents according to the five categories described above (35). For each category, reagents occurred in the sparse matrix with a frequency proportional to the number of times

that reagent produced tRNA crystals. These reagents were then randomly shuffled using the program EXCEL (Microsoft), and a set of 44 conditions was generated. Five different pH values were chosen, along with appropriate buffers: potassium succinate, pH 5.5; potassium cacodylate, pH 6.0; potassium Pipes, pH 6.5; potassium Mops, pH 7.0; potassium Hepes, pH 7.5; Tris·HCl, pH 8.0; each buffer chemical has proven to be suitable for tRNA crystallization. The choice of polyamine, magnesium, and other divalent metal ion concentrations was biased according to those used for tRNAs. Precipitating agents are listed in Table 1. The resulting sparse matrix for RNA crystallization trials is shown in Table 2.

Growth of Crystals. The sparse matrix of crystallization conditions was used to screen for crystal growth with 10 different RNA molecules (Table 3). Crystals were obtained at 22°C. Conditions that produced crystals were then optimized by varying the concentration of each reagent in the crystallization drop individually while keeping all other reagents the same. This yielded information about the parameters critical for crystallization, which were then further optimized in the same manner. Since most of the RNA molecules tested crystallized in only one condition in the sparse matrix, it was generally not possible to infer critical crystallization parameters from the results of the sparse matrix alone.

We made several observations during the course of these experiments regarding general procedures for handling the RNA prior to and during crystallization, which differ from methods used for working with proteins. The preincubation of the RNA in buffer and a low concentration of magnesium chloride prior to use in crystallization trials proved to be extremely important for crystal growth. In some cases, crystals were not obtained if preincubation was not performed; in other cases, the size of the crystals varied depending on the preincubation procedure. This procedure was optimized for each RNA tested. In general, optimal preincubation included magnesium concentrations of 5–20 mM magnesium chloride at temperatures of 50°C–60°C. Although heating the RNA in the presence of magnesium caused a small amount of RNA degradation (as analyzed by analytical PAGE), this did not seem to interfere with crystallization. Higher or lower amounts of magnesium, or higher temperature, often caused the RNA to precipitate during the preincubation.

Two of the RNA crystals obtained with the sparse matrix were found to be extremely temperature dependent for growth. The dodecamer duplex was optimized for growth at 37°C; the P4–P6 domain of the *Tetrahymena* intron was optimized for growth at 30°C. The diffraction pattern for each of these crystals was also found to be highly temperature sensitive; changes of only 3° were enough to significantly reduce the maximum resolution of diffraction for P4–P6.

Preliminary Analysis of Crystals. The crystallization conditions of several RNA molecules were optimized to yield crystals substantially larger than those produced in the initial sparse matrix screen. Two of these have been analyzed for x-ray diffraction, and diffraction data have been collected. These results are discussed in more detail below.

P4–P6 domain from the Tetrahymena *intron.* Extensive biochemical evidence suggests that this 160-nucleotide region of the group I intron from *Tetrahymena* forms an independently folded domain within the molecule (40, 44). The domain contains part of the conserved catalytic core of the intron, although it is not active by itself. The tertiary structure of this domain appears to involve long-range contacts, which are maintained in the absence of the other sequences that compose the catalytic core. Deletion studies have shown that when a portion of the domain is removed from the intron, the rate of self-splicing is diminished. Efficient self-splicing is restored when the deleted portion of the domain is supplied to the rest of the intron in trans (45). Thus, this domain forms a structure within the active molecule that is essential for function.

The domain was synthesized by *in vitro* transcription of a plasmid template and purified on denaturing polyacrylamide gels (see *Materials and Methods*). Crystalline precipitate was observed in sparse matrix conditions 4, 8, 19, 20, 22, 25, 26, 33, 34, and 40; small crystals were obtained in condition 24. We generated a second-order sparse matrix to further explore the conditions that produced crystalline precipitate. The second-order sparse matrix consisted of 40 conditions that sampled 2.0–3.5 M ammonium sulfate or 10–40% 2-methyl-2,4-pentanediol (MPD) as precipitants; 1.5–3.75 mM spermine; 2–4 mM CaCl₂, CoCl₂, CrCl₂, NiCl₂, or SrCl₂; 10–40 mM MgCl₂; and pH 5.5–8.0. Although many of these conditions produced crystalline precipitates, no larger crystals were obtained. While the second-order sparse matrix did not aid the search for crystallization conditions for P4–P6, the concept may prove useful with other molecules.

Crystals of P4–P6 appropriate for x-ray diffraction analysis were produced through optimization of condition 24. The

Table 3. Results with RNA molecules tested in the sparse matrix

RNA molecule	Ref.	No. of residues	Crystallization conditions	Notes
Group I intron from *Anabaena*, L-8	36	240	None	
Group I intron from *Azoarcus*	37	162	33, 36	Hexagonal prisms, 20 × 20 × 20 μm; optimized to 100 × 60 × 60 μm
Group I intron *sunY* from bacteriophage T4	38	208	8	Needles, 120 × 5 × 5 μm
Group I intron from *Tetrahymena*, L-21a	39	380	None	
P4–P6 domain from *Tetrahymena* group I intron	40	161	24	Bipyramidal prisms, 120 × 120 × 120 μm; optimized to 300 × 300 × 400 μm
tRNA-Phe derivative	41	62	3	Needle clusters
Leadzyme LZ2	42	30	14	Cubic prisms, 10 × 10 × 10 μm; optimized to 160 × 160 × 160 μm
Leadzyme LZ4	42	12 + 10	10, 16, 17, 21, 28	Needles; spherulites
Pseudoknot	43	28	5, 7	Needles 10 × 10 × 100 μm; optimized to 100 × 100 × 100 μm
12-mer		12	1, 5, 6, 8, 11, 12, 13, 15, 16, 18, 20, 21, 22, 27, 28, 32, 33, 39, 43, 44	Up to 400 × 400 × 400 μm

largest of these measures 300 × 300 × 400 μm. Two crystal forms were obtained under similar conditions—one is monoclinic with unit cell dimensions $a = 73.4$ Å, $b = 145.5$ Å, $c = 192.3$ Å, $\alpha = 90.0°$, $\beta = 137.7°$, $\gamma = 90.0°$; the other is orthorhombic with unit cell dimensions $a = 76.4$ Å, $b = 128.7$ Å, $c = 145.3$ Å, $\alpha = \beta = \gamma = 90.0°$.

The crystals were grown, handled, and analyzed at 30°C. The optimal growth conditions were 20% MPD/20 mM $MgCl_2$/50 mM potassium cacodylate, pH 6.0. Crystals were observed to grow at 22°C but more slowly and to a smaller final size. Some crystals grown at 30°C cracked when moved to 22°C, even for brief periods of time (<10 min). Analysis of x-ray diffraction from the crystals was carried out on a Siemens area detector at 30°C. An experiment was performed to test the temperature sensitivity of the crystals during data collection. Area detector still images were recorded as the temperature of a monoclinic crystal was lowered from 30°C to 17.5°C in 2.5°C increments. Diffraction diminished steadily until at 17.5°C nearly all reflections were gone. Next, the crystal temperature was adjusted back to 30°C in 2.5°C increments, and at 30°C the original pattern of reflections was observed. Temperatures higher than 30°C also resulted in loss of reflections.

Through use of cryocooling techniques, diffraction to 2.8 Å resolution has been measured from orthorhombic crystals (unpublished data). Fig. 1 shows a 1° oscillation data frame for an orthorhombic crystal of the P4–P6 domain. A native data set has been collected to this resolution; searches for heavy atom derivatives remain to be done.

Twelve-residue oligonucleotide. The oligonucleotide sequence 5'-pGGCGCUUGCGCC-3' forms either a hairpin or a duplex structure in solution (data not shown). The equilibrium between these two conformations is highly salt dependent, with the hairpin favored only in the absence of salt. This molecule was synthesized initially by *in vitro* transcription of a DNA oligonucleotide template and purified by denaturing PAGE.

As shown in Table 3, crystals were obtained in approximately half the conditions of the sparse matrix. Optimization of crystallization in ammonium sulfate (1 M ammonium sulfate/5–20 mM $MgCl_2$/potassium cacodylate, pH 6.0;
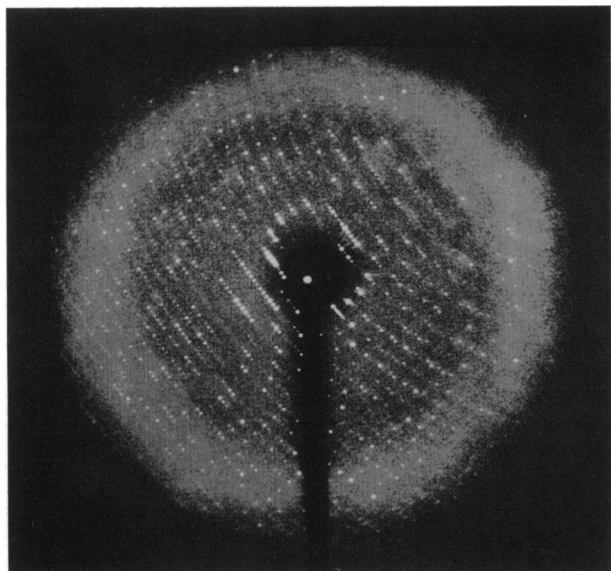

FIG. 1. A 1° oscillation data frame for P4–P6 crystal. Reflections were observed to 2.8-Å resolution from an orthorhombic P4–P6 crystal. The crystal was cryocooled in liquid propane using techniques developed by David Jeruzalmi (personal communication) and analyzed under a stream of N_2 gas at −174°C. Data were collected with an R-Axis II area detector equipped with focusing mirrors.

37°C) yielded crystals suitable for x-ray diffraction analysis. The crystals belong to space group P1 and have unit cell dimensions $a = 31.4$ Å, $b = 32.2$ Å, $c = 46.1$ Å, $\alpha = 106.7°$, $\beta = 78.6°$, $\gamma = 94.5°$. A 3-Å data set has been collected.

Conclusions. RNA molecules of varying size and sequence, synthesized *in vitro*, can be crystallized and studied by x-ray diffraction analysis. The sparse matrix method presented for RNA crystallization is rapid and economical, thus allowing variables such as sequence and preannealing conditions to be explored. Using this method, we have crystallized eight RNA molecules ranging from 12 nucleotides to >200 nucleotides long. Several of these crystals are now in various stages of data collection and processing. The solution of the crystal structures of these RNA molecules and others will have broad implications for the understanding of RNA folding and catalysis at a detailed molecular level. The authors welcome comments from other investigators regarding crystallization of additional RNA molecules using our sparse matrix approach.

1. Cech, T. R. (1987) *Science* **236**, 1532–1539.
2. Celander, D. W. & Cech, T. R. (1991) *Science* **251**, 401–407.
3. Haas, E. S., Morse, D. P., Brown, J. W., Schmidt, F. J. & Pace, N. R. (1991) *Science* **254**, 853–856.
4. Uhlenbeck, O. C., Dahm, S. C., Ruffner, D. E. & Fedor, M. J. (1989) *Nucleic Acids Symp. Ser.* **1989**, 95–96.
5. Doudna, J. A., Cormack, B. P. & Szostak, J. W. (1989) *Proc. Natl. Acad. Sci. USA* **86**, 7402–7406.
6. Michel, F., Hanna, M., Green, R., Bartel, D. P. & Szostak, J. W. (1989) *Nature (London)* **342**, 391–395.
7. Pyle, A. M., Murphy, F. L. & Cech, T. R. (1992) *Nature (London)* **358**, 123–128.
8. Been, M. D. & Perrotta, A. T. (1991) *Science* **252**, 434–437.
9. Hou, Y. M. & Schimmel, P. (1988) *Nature (London)* **333**, 140–145.
10. Rould, M. A., Perona, J. J., Soll, D. & Steitz, T. A. (1989) *Science* **246**, 1135–1142.
11. Feng, S. & Holland, E. C. (1988) *Nature (London)* **334**, 165–167.
12. Selby, M. J., Bain, E. S., Luciw, P. A. & Peterlin, B. M. (1989) *Genes Dev.* **3**, 547–558.
13. Malim, M. H., Hauber, J., Le, S. Y., Maizel, J. V. & Cullen, B. R. (1989) *Nature (London)* **338**, 254–257.
14. Bartel, D. P., Zapp, M. L., Green, M. R. & Szostak, J. W. (1991) *Cell* **67**, 529–536.
15. Puglisi, J. D., Tan, R., Calnan, B. J., Frankel, A. D. & Williamson, J. R. (1992) *Science* **257**, 76–80.
16. Michel, F. & Westhof, E. (1990) *J. Mol. Biol.* **216**, 585–610.
17. Gutell, R. R. & Woese, C. R. (1990) *Proc. Natl. Acad. Sci. USA* **87**, 663–667.
18. Green, R., Ellington, A. D. & Szostak, J. W. (1990) *Nature (London)* **347**, 406–408.
19. Robertson, D. L. & Joyce, G. F. (1990) *Nature (London)* **344**, 467–468.
20. Robertus, J. D., Ladner, J. E., Finch, J. R., Rhodes, D., Brown, R. S., Clark, B. F. & Klug, A. (1974) *Nature (London)* **250**, 546–551.
21. Schevitz, R. W., Podjarny, A. D., Krishnamachari, N., Hughes, J. J., Sigler, P. B. & Sussman, J. L. (1979) *Nature (London)* **278**, 188–190.
22. Basavappa, R. & Sigler, P. B. (1991) *EMBO J.* **10**, 3105–3111.
23. Kim, S. H., Suddath, F. L., Quigley, G. J., McPherson, A.,

Sussman, J. L., Wang, A. H. J., Seeman, N. C. & Rich, A. (1974) *Science* **185**, 435–440.

24. Holbrook, S. R., Cheong, C., Tinoco, I. J. & Kim, S. H. (1991) *Nature (London)* **353**, 579–581.
25. Dock-Bregeon, A. C., Chevrier, B., Podjarny, A., Johnson, J., de Bear, J. S.,Gough, G. R., Gilham, P. T. & Moras, D. (1989) *J. Mol. Biol.* **209**, 459–474.
26. Fedor, M. J. & Uhlenbeck, O. C. (1990) *Proc. Natl. Acad. Sci. USA* **87**, 1668–1672.
27. Kao, T. H. & Crothers, D. M. (1980) *Proc. Natl. Acad. Sci. USA* **77**, 3360–3364.
28. LeCuyer, K. & Crothers, D. M. (1993) *Biochemistry*, in press.
29. Carter, C. J. & Carter, C. W. (1979) *J. Biol. Chem.* **254**, 12219–12223.
30. Jancarik, J. & Kim, S. H. (1991) *J. Appl. Crystallogr.* **24**, 409–411.
31. Milligan, J. F. & Uhlenbeck, O. C. (1989) *Methods Enzymol.* **180**, 51–62.
32. Usman, N., Ogilvie, K. K., Jiang, M. Y. & Cedergren, R. L. (1987) *J. Am. Chem. Soc.* **109**, 7845–7854.
33. Usman, N., Nicoghosian, K., Cedergren, R. L. & Ogilvie, K. K. (1988) *Proc. Natl. Acad. Sci. USA* **85**, 5764–5768.
34. McPherson, A. (1990) *Eur. J. Biochem.* **189**, 1–23.
35. Dock, A. C., Lorber, B., Moras, D., Pixa, G., Thierry, J. C. & Giege, R. (1984) *Biochimie* **66**, 179–201.
36. Xu, M. Q., Kathe, S. D., Goodrich, B. H., Nierzwicki, B. S. & Shub, D. A. (1990) *Science* **250**, 1566–1570.
37. Reinhold, H. & Shub, D. A. (1992) *Nature (London)* **357**, 173–176.
38. Doudna, J. A. & Szostak, J. W. (1989) *Mol. Cell. Biol.* **9**, 5480–5483.
39. Grosshans, C. A. & Cech, T. R. (1991) *Nucleic Acids Res.* **19**, 3875–3880.
40. Murphy, F. L. & Cech, T. R. (1993) *Biochemistry* **92**, 5291–5300.
41. Dichtl, B., Pan, T., DiRenzo, A. B. & Uhlenbeck, O. C. (1993) *Nucleic Acids Res.* **21**, 531–535.
42. Pan, T. & Uhlenbeck, O. C. (1992) *Nature (London)* **358**, 560–563.
43. Tuerk, C., MacDougal, S. & Gold, L. (1992) *Proc. Natl. Acad. Sci. USA* **89**, 6988–6992.
44. Latham, J. A. & Cech, T. R. (1989) *Science* **245**, 276–282.
45. van der Horst, G., Christian, A. & Inoue, T. (1991) *Proc. Natl. Acad. Sci. USA* **88**, 184–188.